HHS Public Access

Author manuscript

Anal Chem. Author manuscript; available in PMC 2016 March 16.

Published in final edited form as:

Anal Chem. 2016 February 2; 88(3): 1728–1733. doi:10.1021/acs.analchem.5b03910.

Mobility-Selected Ion Trapping and Enrichment Using Structures for Lossless Ion Manipulations

Tsung-Chi Chen, **Yehia M. Ibrahim**, **Ian K. Webb**, **Sandilya V. B. Garimella**, **Xing Zhang**, **Ahmed M. Hamid**, **Liulin Deng**, **William E. Karnesky**, **Spencer A. Prost**, **Jeremy A. Sandoval**, **Randolph V. Norheim**, **Gordon A. Anderson**, **Aleksey V. Tolmachev**, **Erin S. Baker**, and **Richard D. Smith***

Biological Sciences Division, Pacific Northwest National Laboratory, Richland, Washington 99352, United States

Abstract

The integration of ion mobility spectrometry (IMS) with mass spectrometry (MS) and the ability to trap ions in IMS-MS measurements is of great importance for performing reactions, accumulating ions, and increasing analytical measurement sensitivity. The development of Structures for Lossless Ion Manipulations (SLIM) offers the potential for ion manipulations in an extended and more effective manner, while opening opportunities for many more complex sequences of manipulations. Here, we demonstrate an ion separation and trapping module and a method based upon SLIM that consists of a linear mobility ion drift region, a switch/tee and a trapping region that allows the isolation and accumulation of mobility-separated species. The operation and optimization of the SLIM switch/tee and trap are described and demonstrated for the enrichment of the low abundance ions. A linear improvement in ion intensity was observed with the number of trapping/accumulation events using the SLIM trap, illustrating its potential for enhancing the sensitivity of low abundance or targeted species.

Graphical abstract

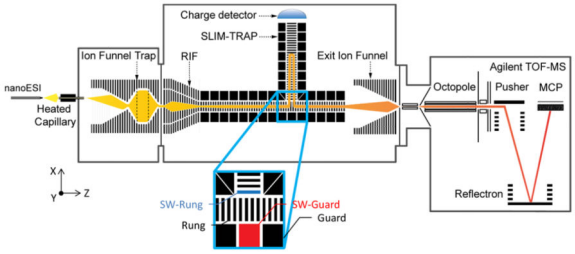

***Corresponding Author**. rds@pnnl.gov.

ASSOCIATED CONTENT

Supporting Information

The Supporting Information is available free of charge on the ACS Publications website at DOI: 10.1021/acs.analchem.5b03910.

Ion trajectories at the conjunction of a SLIM tee; mass spectra (PDF)

The authors declare no competing financial interest.

Increases in the sensitivity and dynamic range of ion mobility spectrometry (IMS)-mass spectrometry (MS) measurements are important for many applications. In conventional pulsed introduction of ions for IMS, only a small portion of the ions from a continuous (e.g., electrospray) ion source contribute to the mobility spectra because of the low duty cycle of transferring a continuous ion beam to pulsed ion packets.[1] Approaches for improving the IMS duty cycle, such as by ion accumulation using the electrodynamic ion funnel trap prior to the IMS-MS analysis, or by multiplexing of releases from the trap, have greatly increased the overall ion utilization efficiency.[2–6] However, sensitivity using the pulsed introduction of ions for IMS ultimately becomes limited by the space charge capacity of traps used to accumulate ions.[7,8]

An alternative approach for improving sensitivity is to accumulate species after an initial separation (e.g., by IMS, MS, liquid or gas phase chromatography) and where space charge effects are generally far less problematic. Selective ion trapping is widely used in mass spectrometry and often utilized for the initial selection of ions in tandem mass spectrometry (MS/MS).[9,10] The ions in the selected *m/z* range are retained while all others are expelled, e.g., by manipulating the ion trapping potential using a forward RF scan[11,12] or applying an additional dipolar excitation waveform, such as a stored waveform inverse Fourier transform (SWIFT),[13] as, e.g., used for the isolation of precursor ions prior to collision-induced dissociation (CID)[14] of targeted ions.[15,16]

Creating effective ion trapping methods between ambient ionization sources (at 760 Torr) and mass spectrometers (generally at $<10^{-4}$ Torr) is of interest. Subambient pressure allows one to exploit conditions that reduce ion losses and facilitate high ion transmission into IMS devices (often functioning at 1 to 10 Torr). The recent development of Structures for Lossless Ion Manipulations (SLIM)[17–22] promises to enable extended sequences of ion manipulations at such pressures. Initially explored SLIM have shown, e.g., utility for ion focusing, transmission, and ease of interfacing to MS.[17,18] This technology has also shown the ability to perform lossless ion mobility separations,[20] ion switching,[21] and ion storage.[19] These capabilities have broad potential utility, such as for the ion enrichment of low concentration targets from high concentration matrix components, or the separation of isomeric species or isobars that typically require ultrahigh mass-resolved spectra.

In the present work, previously developed SLIM components are integrated to provide a combined ion separations and trapping module. A SLIM IMS stage and a trap with axial DC field control was fabricated to create effective ion trapping regions and combined with a SLIM switch, to enable the trapping and accumulation of mobility selected ions. In this work, we demonstrate that the separation and switching provided precise ion selectivity, allowing significant improvements in sensitivity with the use of multiple trap accumulation steps.

EXPERIMENTAL SETUP

Instrumentation

As shown in Figure 1, positive ions generated from an ESI source (3 kV, ambient pressure) were initially introduced through a heated capillary (140 °C, 500 μm i.d., and 10 cm long) to

an ion funnel trap (3.99 Torr). The capillary had a 10 mm offset from the ion funnel trap centerline to reduce downstream pressure and largely eliminate contamination of the SLIM with species not effectively confined by the RF used for the ion funnel and thus built up on surfaces of the SLIM module. The ion funnel trap (IFT) was utilized in this initial work[5,23] and a rectangular ion funnel (RIF)[24] after the IFT to provide efficient transmission of ions into the SLIM drift region. Details of the SLIM-TOF MS configuration have been given previously.[20,21,24] The entire SLIM module in this study consists of a 38 cm long linear drift region, a switch (SW; "tee"), and a 27 cm trap region located orthogonal to the drift region. The two mirror-image electrode surfaces of the SLIM module were spaced 4.6 mm apart (*y*-direction, Figure 1). The electric field providing confinement between symmetric planes was produced from the DC-only guard electrodes in conjunction with the DC/RF coupling rung electrodes (180° phase shifted between adjacent electrodes) along the entire ion path. Switching times for potential changes on the switching rung electrode (i.e., SW-Rung, the first rung electrode on the trap, blue bar in Figure 1 inset) and switching guard electrode (SW-Guard, red square in Figure 1 inset) were precalibrated by measuring the arrival time of the targets from the IFT to the tee. A diagram of the detailed control sequence for the ion switching and trapping is given in Figure 2a. Accumulated ion packets were injected from the IFT into the RIF-SLIM module according to a predefined pulse sequence (Figure 2a). During the ion injection into the SLIM trap (Figure 2b top panel), the potential on the SW-rung electrode was set lower than the SW-guard electrode to create a field that directs ions to the SLIM trap. The potential on the SW-rung electrode was later returned to the original level (Figure 2b middle panel) to prevent undesired ions from entering the trap. The delay as well as the width of switching pulses were calibrated according to the arrival time and the desired packet size.[22] The gating and switching operations could be repeated an arbitrary number of times, and each iteration resulted in one additional SLIM trap ion accumulation step. After the termination of ion accumulation, the potentials applied at the end of the trap were raised in order to create a repulsive force to eject ions. The data acquisition was triggered when ions were released from the IFT to record the ions arrival time after the release from the accumulation trap, instead of their IMS drift time.

Ions exiting the SLIM module were radially refocused by another ion funnel to provide efficient transmission through the differential pressure interfaces of the TOF-MS (model 6224, Agilent Technologies, Santa Clara, CA). DC gradients of the RIF, linear SLIM module, and the exit IF were all set to 10 V/cm, and the DC guard of the whole SLIM module was biased 5 V higher than adjacent central rung voltages. The IFT was operated at 0.8 MHz and 160 V_{pp}, while the exit funnel was operated at 0.8 MHz and 140 V_{pp}. The RF amplitude of the short quadrupole (Q0) behind the exit ion funnel was 124 V_{pp} at 1.2 MHz, and the SLIM module RF was at 0.8 MHz and 200 V_{pp}.

Acquisition

IMS and MS data was acquired with a U1084A 8-bit analog-to-digital converter (U1084A 8-bit, Keysight Technologies, Santa Rosa, CA) using home-built control software. All data presented in this work utilizes triplicate analyses in order to calculate the mean and the standard deviation.

Chemicals and Materials

Chemicals used in this study included the ESI-L low concentration tune mix (Agilent Technologies, Santa Clara, CA) and an equimolar nine peptide mixture. The tune mix was used to produce singly charged ions with *m/z* range from 118.09 to 2721.89 in ESI positive mode for the SLIM system optimization. The mixture of 9 peptides, all purchased from Sigma-Aldrich (St. Louis, MO), included bradykinin (MW 1060.21), human angiotensin I (MW 1296.48), human neurotensin (MW 1672.92), fibrinopeptide A (MW 1536.56), substance P (MW 1347.63), kemptide (MW 771.91), angiotensin II (MW 1046.18), melittin (MW 2846.46), and renin (MW 1759.01). Each peptide in the mix was prepared to a concentration of 200 nM in 1:1 (vol/vol) water/methanol with 0.1% acetic acid (Fisher Scientific, Pittsburgh, PA).

RESULTS AND DISCUSSION

The efficiency of ion switching in the SLIM relies on precise timing of the switch potentials in order to direct the targeted mobility (e.g., a selected IMS peak) to an orthogonal path. The characterization of the switching times has been previously demonstrated.[22] However, the adaptation of the SLIM trap to the SLIM switch represents a major departure from in-line SLIM trapping[19] as the electric fields at the exit of the trap will affect the efficiency of trap due to field penetration into the trapping region of turning potentials and vice versa. Therefore, it is necessary to further refine and optimize the ion injection, trapping, and release steps. Ion injection and trapping are obviously affected by the DC gradient in the SLIM trap. Due to the repulsive and attractive fields applied to the switching electrodes, ions are initially accelerated as they enter the SLIM trap. During injection into the SLIM trap, ions are decelerated by the repulsive potential gradient in the first trapping zone ($\overline{\mathrm{RA}}$ in Figure 2b, first panel). After ion injection, a potential well for axial confinement is required to maintain the ion population for long trapping periods (>seconds). For these experiments, an appropriate field distribution in the trap (middle, Figure 2b) was used to provide the confinement in the axial direction and to cause ions to be repelled toward the bottom of the trap (point A, Figure 2b). The resulting ion packet is squeezed, decreasing the initial ion pulse width as it is released from the trap. High DC gradients, however, were found to lower the trapping capacity of the SLIM trap. Figure 3a shows the signal intensity as a function of the DC gradient along zone $\overline{\mathrm{AB}}$ of the trap (see Figure 2b). Only *m/z* 622 ions from the tune mix were selected and trapped. The DC gradient at $\overline{\mathrm{RA}}$ was fixed at 5 V/cm during the ion trapping, and the DC gradient at $\overline{\mathrm{RB}}$ was 8 V/cm during release. The RF and the DC field at the in-line path were configured, as described in the Experimental Setup. The greatest signal intensity was obtained at a DC gradient of 0.2 V/cm on $\overline{\mathrm{AB}}$. Decreased ion signals were observed when the gradient was changed from 0.2 to 1 V/cm, since the trapping space is progressively limited due to space charge effects. The decreased trap capacity at higher DC gradients was also observed previously in the ion funnel trap.[5] During ion release, the DC gradient in the trap was altered to create a reversed field in order to eject ions to the in-line path (Figure 2b). As ions were ejected axially, they experienced a repulsive force at the tee junction from the SW-guard electrode combined with the original in-line DC field that guides ions toward the MS. We note that the shuttling of ion packets around the corner can be affected by the releasing gradient. With fixed RF confinement on a SLIM tee, a strong

releasing gradient reduces the ion transmission efficiency, while a more “gentle” gradient produces better transmission but a more extended ion packet. Figure 3b shows the effect of the release DC field in the SLIM trap on the ion transmission and the full width at half-maximum (fwhm) of the released ion packet. In this experiment, the trapping gradient was fixed at 5 V/cm and other experimental conditions are adopted on the basis of the optimization results in the previous sections. The greatest observed signal was obtained using a releasing gradient of 1 V/cm yielding a fwhm of 17.6 ms (Figure 3b inset). In contrast, a much narrower peak was obtained using a releasing gradient of 8 V/cm (fwhm 2.7 ms, Figure 3b inset), however, with ~1/3 less peak area compared to the 1 V/cm. Increasing the releasing gradient above 9 V/cm further significantly reduces ion intensities, as seen in Figure 3b. The ion losses observed at high gradients are attributed to the increased orthogonal component of the electric field (i.e., toward the electrodes), which is created at the trap exit, where the linear gradient transitions into an effectively flat potential profile. An orthogonal field increase at the junction is supported by potential calculations and consideration of Gauss’s law,[25] which requires a balance of the net electric flux through a closed surface. The orthogonal field propels ions toward the surfaces and is offset by the effective potential generated by RF applied to rung electrodes[17] and where higher RF confinement is needed for high releasing gradients, resulting in some ion losses.[21] Therefore, under the conditions used in this study, the highest sensitivity (i.e., transfer efficiency, measured by the integrated area of the mobility peak) was achieved at ~1 V/cm, and it was not our aim to minimize the size of the ejected packet after selection and trapping. However, we note that ejection with higher gradients results in narrower peaks. While the highest achievable RF confinement is limited by electrical breakdown and the constraints of the RLC resonant circuit, increased RF amplitude is expected to allow greater releasing gradients and provide efficient ion transmission along with more focused (i.e., narrow) ion packets. Alternatively, the SLIM-trap design can be modified such that the DC gradient is terminated prior to the tee junction, so the ions travel some distance before entering the tee junction.

Next, the ion storage limits of the SLIM trap were evaluated. Tune mix ions were first accumulated in the IFT for 4 ms[5,23] and then injected into the linear region of the SLIM module (34.3 cm total, including the RIF). Figure 4a shows the arrival time distribution for ions released from the IFT with no accumulation in the SLIM trap. The three peaks were baseline separated with ~5.3 ms difference. The switch potentials were activated for a period ($t - t_0$) of 25.9 to 29.3 ms after the ions were released from the IFT. Only the mobility peaks of *m/z* 922.0 and 1223.0 were detected at the TOF MS since the mobility peak of *m/z* 622.0 was switched into the trap (Figure 4b). The switching sequence (Figure 2b) was repeated multiple times, while ions were held in the SLIM trap, to accumulate only *m/z* 622.0 ions in the SLIM trap. Following the accumulation step, the direction of the field in the trap was reversed and trapped *m/z* 622.0 ions were released to the TOF MS for detection (Figure 4c; note that the data acquisition ion arrival time shown, ~4090 ms, is referenced to the time ions are initially released from the IFT). The comparison of the integrated peak areas corresponding to *m/z* 622.0 ions between Figure 4a and c gives a total efficiency of switching, trapping, and releasing of >95%. To investigate the limits of the trap, the number of ion accumulations was varied, as shown in Figure 4d. The experimental parameters were

optimized according to the previous characterization results. The signal for the third isotopic peak (*m/z* 624.0) was utilized to avoid detection bias caused by detection saturation due to the limited dynamic range of the ADC. These results indicate a nearly linear increase up to 175 accumulations and a plateau beyond 175 accumulations as the trap reached its capacity. Similar results (Figure 5a–f) were obtained for enriching the low abundant ions of melittin 4+ (*m/z* 712.48) from a mixture of 9 peptides. Figure 5a–d shows the mass spectrum and the arrival time distribution, respectively, of the 9 peptide mixture. The switch was activated from 24.4 to 24.7 ms, which correlates with the arrival time of melittin 4+ ions to the switch region (the shaded area in Figure 5d). Ions that were not switched arrived at the TOF as shown in Figure 5b,e, consistent with notching of the targeted peak. The trapped ions were released from the SLIM trap after 100 switching and accumulations for detection, as shown in Figure 5c–f. The efficiency of this experiment over the switching time used was 100% to within measurement uncertainty for the targeted melittin ions. The mass spectrum shown in Figure 5c contains additional peaks due to the limited IMS resolution achieved in the present module due to the short SLIM region prior to the switch and thus some overlap with the targeted peak. However, the overlap of peaks is not due to the performance of the switch itself. Instead, improving resolution by extending the mobility separation before the switch will minimize overlap, such as observed in Figure 5c, and separate the ions to the extent that individual components can be switched.

CONCLUSIONS

In this work, the switching and trapping of mobility-selected ions at 4 Torr of nitrogen was demonstrated using an integration of an IMS drift region, tee, and trap area based on SLIM technology. The different potentials in the SLIM module were optimized to obtain efficient ion transmission in the switching and trapping regions. Ion switching potentials for SW-rung were found to be ideal at ~20 to 30 V lower than the potentials in the “no trapping” mode. Trapping efficiency was determined to be optimal when a low DC gradient was used in the trapping region. Lower DC gradients were also found to be the best for the ion ejection transmission. Finally, ion accumulation showed that the SLIM trap can store and accumulate selected ions up to the maximum capacity of the trap. Improvements to the trap design should further enhance the performance of the SLIM trap and provide the basis for more complex SLIM, e.g., using multiple traps or introducing reaction steps prior to additional IMS separations.

Supplementary Material

Refer to Web version on PubMed Central for supplementary material.

Acknowledgments

Portions of this work were supported by the National Institute of General Medical Sciences (P41 GM103493), the Laboratory Directed Research and Development (LDRD) program at Pacific Northwest National Laboratory, and the Department of Energy Office of Biological and Environmental Research Genome Sciences Program under the Pan-omics Program. Experiments were performed in the Environmental Molecular Science Laboratory (EMSL), a U.S. Department of Energy (DOE) national scientific user facility at Pacific Northwest National Laboratory (PNNL) operated by Battelle for the DOE under contract DE-AC05-76RL0 1830.

REFERENCES

1. Knorr FJ, Eatherton RL, Siems WF, Hill HH. Anal. Chem. 1985; 57:402–406. [PubMed: 3977072]
2. Ibrahim Y, Belov ME, Tolmachev AV, Prior DC, Smith RD. Anal. Chem. 2007; 79:7845–7852. [PubMed: 17850113]
3. Wyttenbach T, Kemper PR, Bowers MT. Int. J. Mass Spectrom. 2001; 212:13–23.
4. Clowers BH, Siems WF, Hill HH, Massick SM. Anal. Chem. 2006; 78:44–51. [PubMed: 16383309]
5. Ibrahim Y, Belov ME, Tolmachev AV, Prior DC, Smith RD. Anal. Chem. 2007; 79:7845–7852. [PubMed: 17850113]
6. Clowers BH, Ibrahim YM, Prior DC, Danielson WF 3rd, Belov ME, Smith RD. Anal. Chem. 2008; 80:612–623. [PubMed: 18166021]
7. Belov ME, Nikolaev EN, Harkewicz R, Masselon CD, Alving K, Smith RD. Int. J. Mass Spectrom. 2001; 208:205–225.
8. Tolmachev AV, Udseth HR, Smith RD. Rapid Commun. Mass Spectrom. 2000; 14:1907–1913. [PubMed: 11013419]
9. March, RE.; Todd, JFJ. Practical Aspects of Ion Trap Mass Spectrometry: Vol. I: Fundamentals of Ion Trap Mass Spectrometry. Vol. 1. Boca Raton, FL: CRC Press; 1995.
10. March, RE. Encyclopedia of Analytical Chemistry. New York: John Wiley & Sons, Ltd.; 2006.
11. Schwartz JC, Jaardine I. Rapid Commun. Mass Spectrom. 1992; 6:313–317.
12. Soni MH, Cooks RG. Anal. Chem. 1994; 66:2488–2496.
13. Guan S, Marshall AG. Anal. Chem. 1993; 65:1288–1294. [PubMed: 8503506]
14. Mitchell Wells J, McLuckey SA. Methods Enzymol. 2005; 402:148–185. [PubMed: 16401509]
15. Blake TA, Ouyang Z, Wiseman JM, Takáts Z, Guymon AJ, Kothari S, Cooks RG. Anal. Chem. 2004; 76:6293–6305. [PubMed: 15516121]
16. Ouyang Z, Takáts Z, Blake TA, Gologan B, Guymon AJ, Wiseman JM, Oliver JC, Davisson VJ, Cooks RG. Science. 2003; 301:1351–1354. [PubMed: 12920304]
17. Garimella SVB, Ibrahim YM, Webb IK, Tolmachev AV, Zhang X, Prost SA, Anderson GA, Smith RD. J. Am. Soc. Mass Spectrom. 2014; 25:1890–1896. [PubMed: 25257188]
18. Tolmachev AV, Webb IK, Ibrahim YM, Garimella SVB, Zhang X, Anderson GA, Smith RD. Anal. Chem. 2014; 86:9162–9168. [PubMed: 25152178]
19. Zhang X, Garimella SV, Prost SA, Webb IK, Chen TC, Tang K, Tolmachev AV, Norheim RV, Baker ES, Anderson GA, Ibrahim YM, Smith RD. Anal. Chem. 2015; 87:6010–6016. [PubMed: 25971536]
20. Webb IK, Garimella SVB, Tolmachev AV, Chen T-C, Zhang X, Norheim RV, Prost SA, LaMarche B, Anderson GA, Ibrahim YM, Smith RD. Anal. Chem. 2014; 86:9169–9176. [PubMed: 25152066]
21. Webb IK, Garimella SVB, Tolmachev AV, Chen T-C, Zhang X, Cox JT, Norheim RV, Prost SA, LaMarche B, Anderson GA, Ibrahim YM, Smith RD. Anal. Chem. 2014; 86:9632–9637. [PubMed: 25222548]
22. Garimella SVB, Ibrahim YM, Webb IK, Ipsen AB, Chen T-C, Tolmachev AV, Baker ES, Anderson GA, Smith RD. Analyst. 2015; 140:6845–6852. [PubMed: 26289106]
23. Belov ME, Prasad S, Prior DC, Danielson WF 3rd, Weitz K, Ibrahim YM, Smith RD. Anal. Chem. 2011; 83:2162–2171. [PubMed: 21344863]
24. Chen T-C, Webb IK, Prost SA, Harrer MB, Norheim RV, Tang K, Ibrahim YM, Smith RD. Anal. Chem. 2015; 87:716–722. [PubMed: 25409343]
25. Serway, RA. Physics for Scientists and Engineers with Modern Physics. 4th. Philadelphia: Saunders College Pub.; 1996.

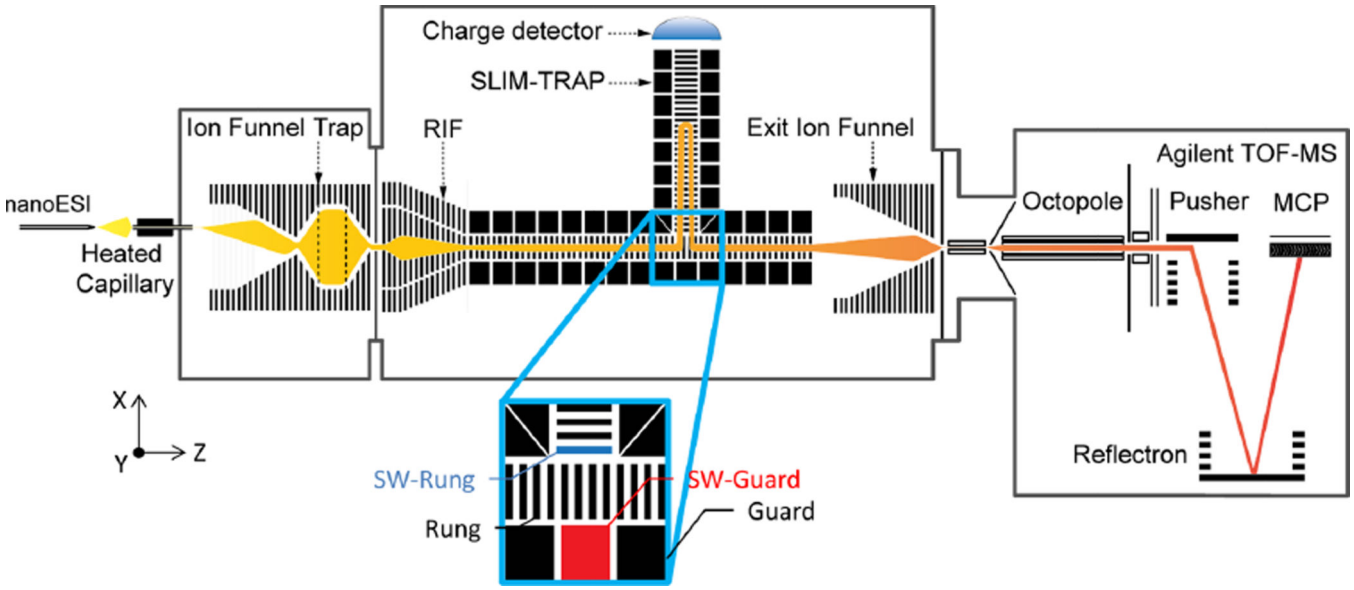

Figure 1.

Schematic diagram of the ESI-SLIM-TOFMS arrangement used in this work and incorporating an orthogonal SLIM trap. The ion switching section is enlarged in the inset.

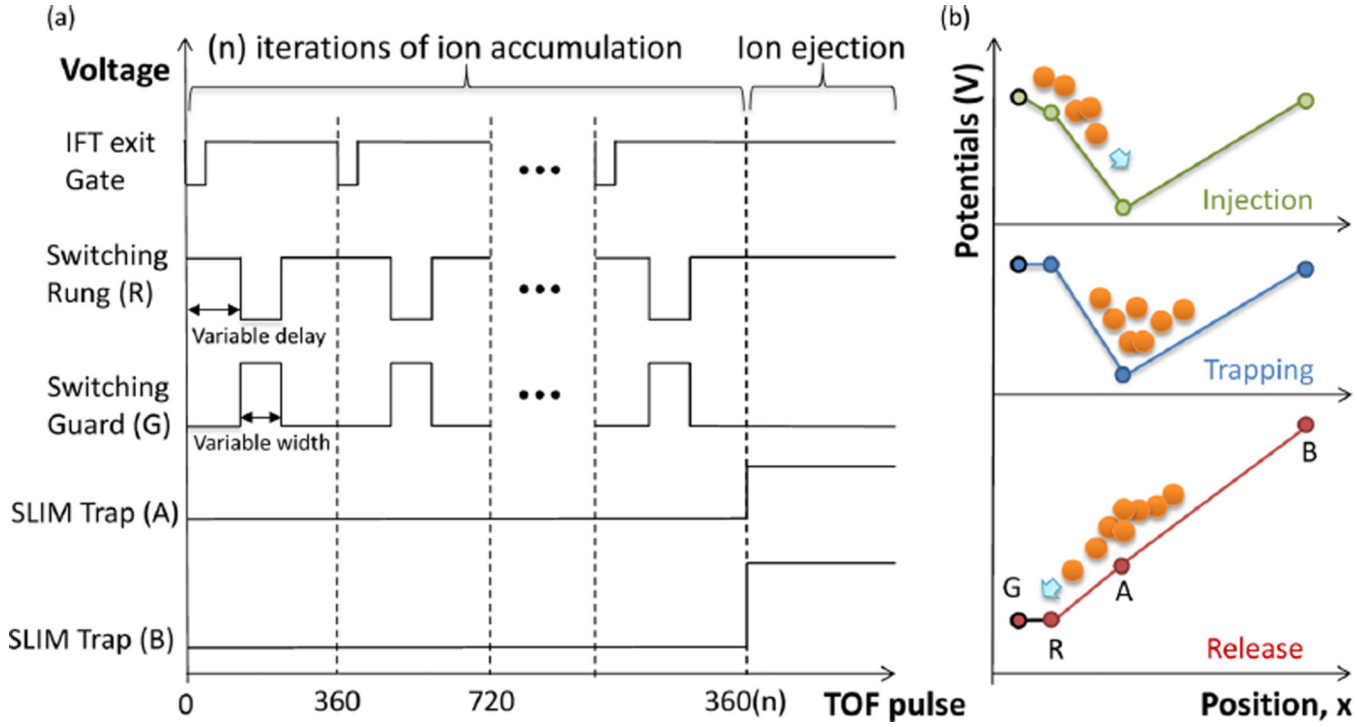

Figure 2.

(a) Control sequences of voltages applied to the exit gate of ion funnel trap, the switch rung, switch guard, SLIM trap valley (point A), and the SLIM trap end (point B). The SLIM trap accumulation and ejection cycle as well as all control signals were synchronized to the TOF pulse. (b) Schematic of the SLIM trap operational potentials for ion injection, trapping, and release.

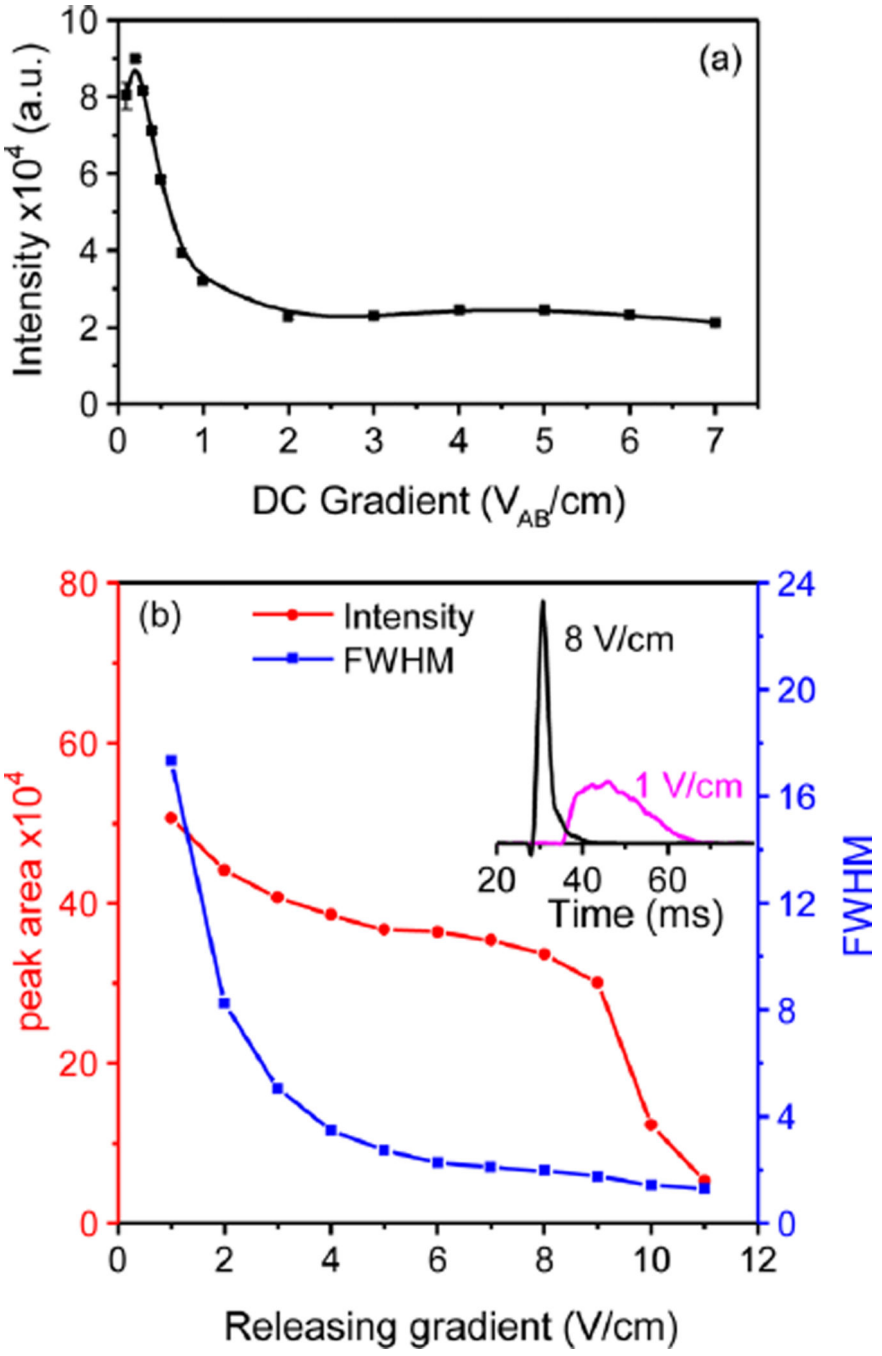

Figure 3.

Measured ion current for different DC gradients during (a) ion trapping and (b) ion release. Red circles and blue squares correspond to the peak area and width at fwhm, respectively. The inset displays the drift time distribution of ions at a DC ejection gradient of 8 V/cm (black) and 1 V/cm (magenta).

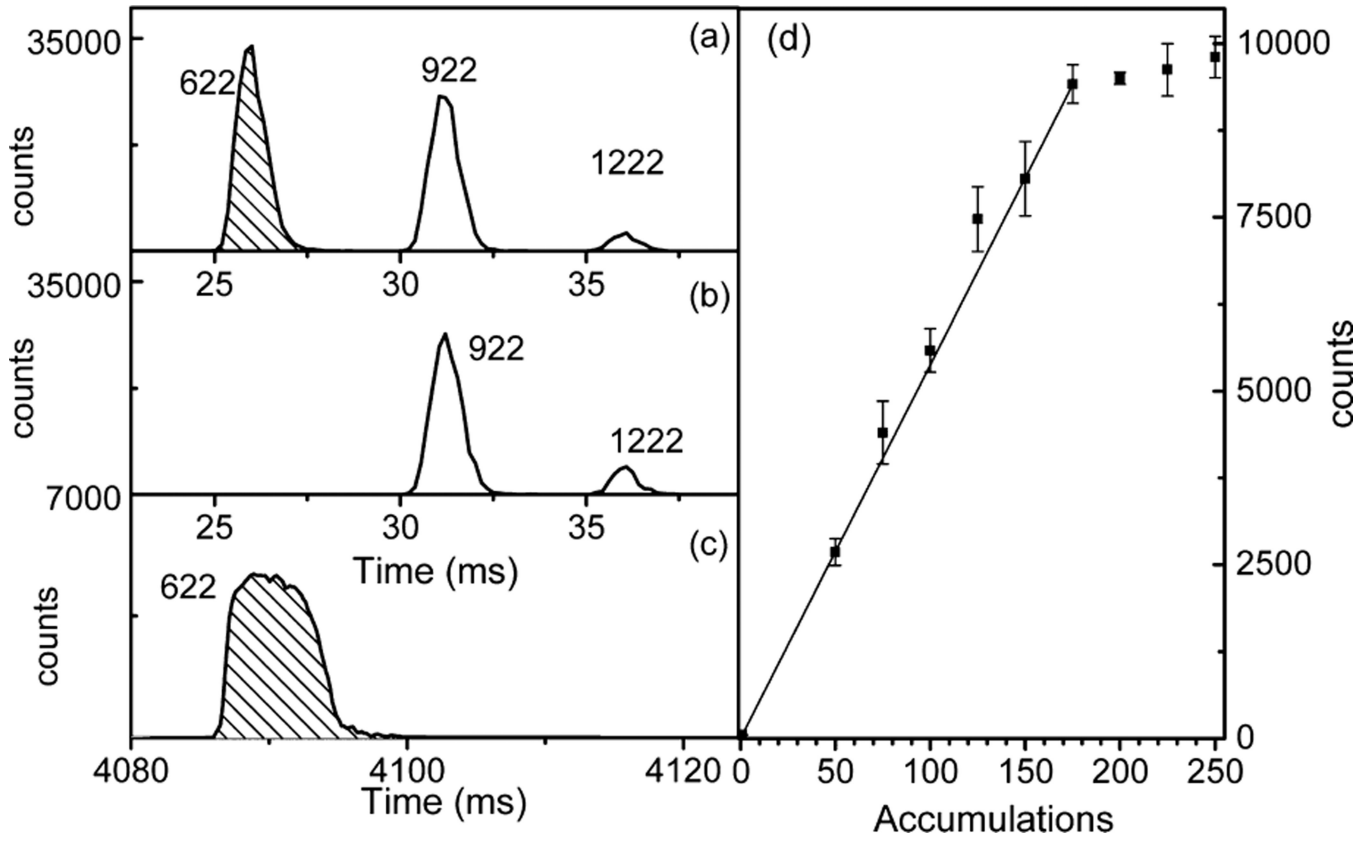

Figure 4.

Arrival time distribution for three peaks of the Agilent tune mix: (a) no trapping in SLIM, (b) ions of *m/z* 622.0 were switched into SLIM, and (c) ions of *m/z* 622.0 were released from SLIM after 100 accumulations. (d) Intensity of the 3rd isotope of *m/z* 622.0 plotted against a number of accumulations in the SLIM trap.

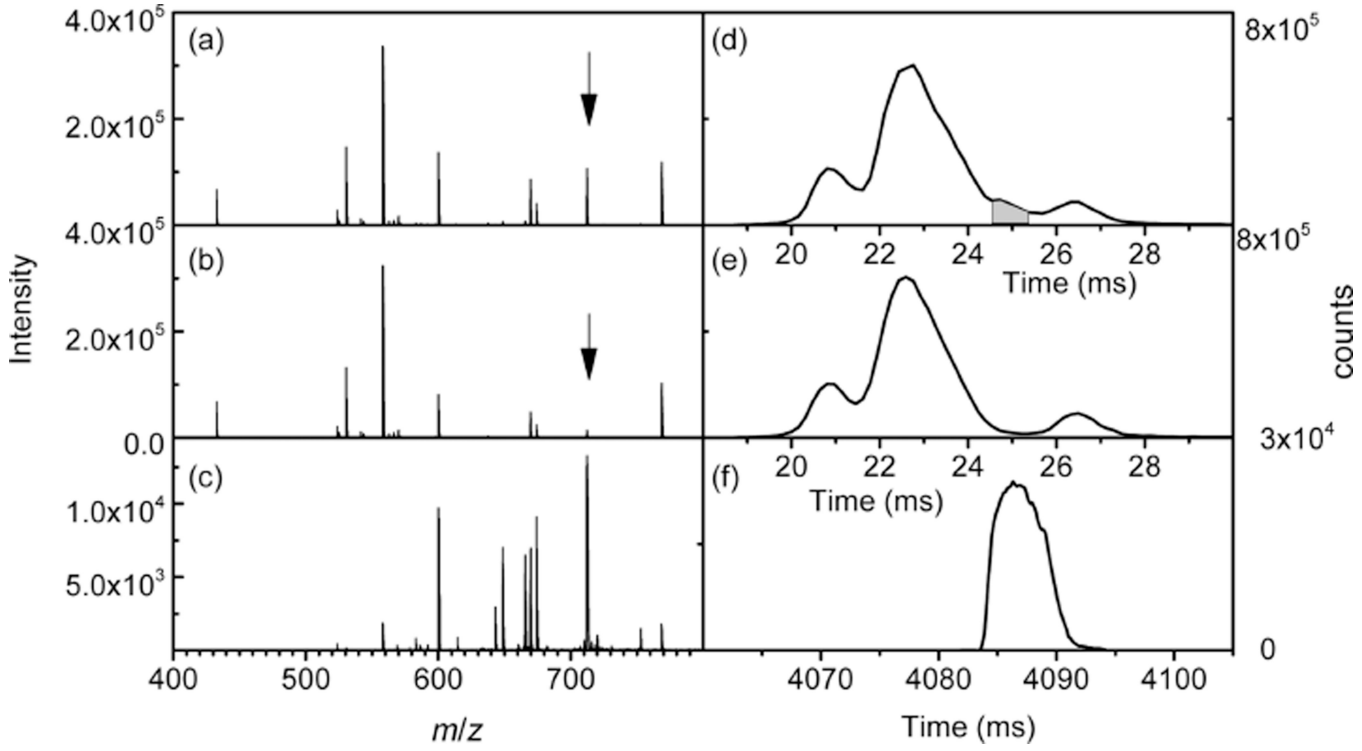

Figure 5.

MS spectra and the corresponding arrival time distributions for a mixture of 9 peptides: (a) and (d) no trapping in SLIM, (b) and (e) ions of *m/z* 712 (melittin 4+ ions) were switched into SLIM, and (c) and (f) ions of *m/z* 712.5 were released from SLIM after 100 accumulations. The shaded area in (d) corresponds to the approximate arrival time of melittin 4+ ions within the 9 peptide mixture. The arrows on panels (a) and (b) point to the melittin 4+ peak (*m/z* 712.5).